TITLE

Hand-selective visual regions represent how to grasp 3D tools for use: brain decoding during real actions

AUTHORS

Ethan Knights[a], Courtney Mansfield[b], Diana Tonin[b], Janak Saada[c], Fraser W. Smith[b], & Stéphanie Rossit[b]

AUTHORS AFFILIATION

[a] MRC Cognition & Brain Sciences Unit, University of Cambridge, UK, CB2 7EF

[b] School of Psychology, University of East Anglia, Norwich NR4 7TJ

[c] Department of Radiology, Norfolk and Norwich University Hospitals NHS Foundation Trust, Norwich NR4 7UY United Kingdom

CORRESPONDING AUTHOR

Stéphanie Rossit, School of Psychology, University of East Anglia, Norwich, NR4 7TJ UK, +44 (0)160359 1674, s.rossit@uea.ac.uk

ABSTRACT

Most neuroimaging experiments that investigate how tools and their associated actions are represented in the brain use visual paradigms where objects and body parts are displayed as 2D images and no real movements are performed. These studies have discovered a tight relationship between hand- and tool-selective areas in LOTC and IPS, thought to reflect action-related processing but this claim has never been directly investigated. Here we addressed this by testing whether independently visually-defined category-selective areas were sensitive to real action properties involving 3D tools. Specifically, using multi-voxel pattern analysis (MVPA), we tested if brain activity patterns would differ depending on whether grasping was consistent or inconsistent with how tools are typically grasped for use (e.g., grasp knife by the handle rather than its serrated edge). In a block-design fMRI paradigm, participants grasped the left or right sides of 3D tools (kitchen utensils) and 3D non-tools (bar-shaped objects) with the right-hand. Importantly, and unknown to participants, by varying movement direction (right/left) the tool grasps were performed in either a typical (by the handle) or atypical (by the functional-end) manner. We found that representations about whether a 3D tool is being grasped appropriately for use were decodable from hand-selective areas (LOTC-Hand and IPS-Hand), but not from tool-, object-, or body-selective areas, even if partially overlapping. These findings indicate that representations of how to grasp tools for use are automatically evoked in visual regions specialised for representing the human hand.

INTRODUCTION

The emergence of handheld tools (such as a spoon) marks the beginning of a major discontinuity between humans and our closest primate relatives (1). A defining feature of tools, compared to other manipulable objects (like a book), is their association with highly predictable motor routines (such as wrist-rotation with a screwdriver; 2). Accurate tool manipulation is generally agreed to result from neurocognitive, rather than musculoskeletal, evolution (3). Yet, in contrast to our understanding of how the human brain represents properties about objects (4,5) or rudimentary hand movements (6,7), little is known about the neural representations that underpin real actions involving 3D tools (8,9,10).

A highly replicable functional imaging finding is that simply viewing pictures of tools activates sensorimotor brain areas, including the premotor cortex and anterior Intraparietal Sulcus (aIPS; e.g., 11,12,13,14), but what drives this functional selectivity? One popular idea is that this visually-evoked activation reflects the automatic retrieval of learnt information about how to act with tools, such as the hand and finger movements needed for their accurate use (11,13,16,17,18,19). Similarly, Supramarginal (SMG) or posterior Middle Temporal Gyri (pMTG) activation for visually presented tools is also often interpreted as indirect evidence that these tool-selective regions are involved in real tool manipulation (e.g., 14,19,20). Nevertheless, we would never grasp a picture of a tool to use it and, more importantly, finding spatially overlapping activation between two tasks does not directly imply that the same neural representations are being triggered (20,21). Thus, whilst embodied views of cognition predict that conceptual tool knowledge is contained (22) or grounded (23,24) in sensorimotor brain areas, the activation of these regions during tool viewing does not necessarily mean that perceiving and acting with tools are neurally instantiated in a similar way (19). In fact, the aIPS activation found when viewing tool pictures versus grasping shows poor correspondence (25,26), questioning the long-standing assumption that visually defined tool areas represent sensorimotor aspects of tool manipulation.

Curiously, the visual regions activated by viewing pictures of human hands in the left IPS (IPS-Hand) and Lateral Occipital Temporal Cortex (LOTC-Hand) overlap with their respective tool-selective areas (IPS-Tool; LOTC-Tool; 27,28,29). Stimulus features often described to drive the organisation of category-selective brain areas, like form (30), animacy (31), texture (32) or manipulability (12) cannot simply explain this shared topography because hands and tools differ on these dimensions. Instead, their overlap is suggested to result from a joint representation of high-level action information related to skilful object manipulation (27,29), perhaps coding the function of hand configurations (33,34,35) or the process by which a tool extends the body's boundaries (28). This account fits with evidence that the LOTC hand/tool region is selectively connected with visuomotor areas such as left aIPS and premotor cortex (27). Further, the existence of this LOTC hand-tool overlap even in individuals who are blind (36) or born without hands (37) suggests that hand- and tool-selective regions may be similar in how they represent abstract non-sensory information about tool manipulation. While the role of visually-defined body-

selective areas in motor control has been the subject of controversy (38,39,40), whether their neighbouring hand-selective areas represent properties of real movements, like the typical way in which tools are manipulated for correct use, remains unknown (41,42). Arguably, the only way to directly test whether these visual tool- or hand-selective areas actually carry information about actions with tools is to examine their responses when participants directly manipulate 3D tools with their hands.

Here, an fMRI experiment involving real hand actions (Fig. 1) tested whether visually defined hand- and tool-selective areas represent how to appropriately grasp 3D tools. Specifically, 19 participants grasped 3D-printed tools in a way that was either consistent with their use (typical: by their handle) or not (atypical: by their functional-end e.g., knife blade). As a control, non-tool bars (adapted from 43) were also grasped on their right or left sides to match as much as possible any biomechanical differences between typical and atypical actions. Multivoxel Pattern Analysis (MVPA) was used to assess whether the different types of grasping for tools (typical vs. atypical) and non-tools (right vs. left), could be decoded using fMRI activity patterns from independent and visually defined Regions of Interest (ROIs). We interpreted greater-than-chance decoding accuracy of typical vs. atypical actions for tools, but not for control non-tools, as evidence that an area contains high-level representations about how a tool should be grasped for its correct use (i.e., by its handle). This pattern of findings was expected only for the tool- and hand-selective areas since these are thought to support accurate tool manipulation (e.g., 16,18,37). Additionally, we performed whole-brain MVPA using searchlight analyses to explore the possibility that this information was encoded by other regions, including those that have previously been shown to process information about hand-object interactions (e.g., 44,45).

RESULTS

For each participant we identified 12 visual ROIs from an independent Bodies, Chairs, Hands and Tools localizer (see Materials and Methods; see Fig. 1D; for ROIs descriptives see Table S1). Given the predominantly left lateralised nature of tool-processing (8), all individual participant ROIs were defined in the left hemisphere (27,28,29,36). Six tool-selective ROIs commonly described in left frontoparietal and occipitotemporal cortices were identified by contrasting activation for tool pictures vs. other object pictures [IPS-Tool; SMG; dorsal and ventral Premotor Cortex (PMd; PMv), LOTC-Tool; pMTG; 11,15). Moreover, two hand-selective ROIs were identified in LOTC (LOTC-Hand) and IPS (IPS-Hand) by contrasting activation for hand pictures vs. pictures of other body parts (27,29,34,35). Additionally, we defined a body-selective (LOTC-Body; Bodies > Chairs; 29), two object-selective ROIs (LOTC-Object; posterior Fusiform, pFs; Chairs > Scrambled; 29,46) and an Early Visual Cortex ROI (EVC; All Categories>Baseline; 29).

In line with our predictions, as can be seen in Fig. 2, Support Vector Machine (SVM) decoding accuracy (false discovery rate-corrected) from hand-selective ROIs in LOTC and IPS

was significantly greater-than-chance when discriminating typical vs. atypical actions with tools, but not non-tools [one-sample t-test against chance 50% - Tools: LOTC-Hand decoding accuracy = 56% ± [SD] 0.9% [$t(16) = 2.73$, $p = 0.007$, $d = 0.66$], IPS-Hand accuracy = 57% ± 0.11% [$t(18) = 2.72$, $p = 0.007$, $d = 0.62$]; Non-tools: both p's > 0.15]. Importantly, results from a stringent comparison (paired samples t-test) of decoding between conditions further supported this: for both LOTC-Hand and IPS-Hand grasp type decoding accuracy was significantly higher for tools than non-tools [LOTC-Hand: $t(16) = 2.11$, $p = 0.026$, $d = 0.51$; IPS-Hand: $t(18) = 3.26$, $p = 0.002$, $d = 0.75$; Fig. 2A and Fig. 2B]. No other visual ROIs, including tool-selective areas, displayed the same pattern of findings. Instead, significant above-chance decoding of grasp type was observed in LOTC-Body and pFs for both tools and non-tools [Tools: LOTC-Body accuracy = 59% ± 0.08% [$t(17) = 4.75$, $p < 0.001$, $d = 1.12$], pFS accuracy = 58% ± 0.14% [$t(18) = 2.57$, $p = 0.01$, $d = 0.59$]; Non-tools: LOTC-Body accuracy = 56% ± 0.10% [$t(17) = 2.46$, $p = 0.012$, $d = 0.58$], pFS accuracy = 57% ± 0.12% [$t(18) = 2.59$, $p = 0.009$, $d = 0.59$]; Fig. 2A]. In addition, PMd decoded actions with non-tools only [accuracy = 59% ± 0.08% [$t(13) = 4.11$, $p = 0.001$, $d = 1.1$], Fig. 2A]. This suggests that hand-selective LOTC and IPS regions represent how to appropriately grasp tools for use. Alternatively, could typical vs. atypical decoding specific for tool stimuli in visual hand-selective cortex be accounted for by low-level differences between the tools' handles and functional-ends? First, to test the possibility that tool-specific decoding in hand-selective cortex could be driven by simple textural differences (e.g., a smooth handle vs. a serrated blade), we repeated the analysis using a left somatosensory cortex ROI (SC; defined by an independent univariate contrast of All Grasps > Baseline; 47). However, unlike the tool specific effects in the hand-selective ROIs, grasp type decoding in SC was significantly greater-than-chance for both tool and non-tools [Tools accuracy = 57% ± 0.11% [$t(18) = 3.04$, $p = 0.004$, $d = 0.7$]; Non-tools accuracy = 57% ± 0.09% [$t(18) = 3.45$, $p = 0.001$, $d = 0.79$]; Fig. 1C], indicating that tool-specific decoding cannot be explained by somatosensory differences in the stimuli. Second, we tested if size differences between our objects, and thus grip size, could drive tool-specific decoding in hand-selective cortex (i.e., the functional-end of the tool being wider than its handle). However, decoding analysis of grip size (i.e., smaller vs. larger) that collapsed across object category (i.e. tools and non-tools) was not was not significant (all p's > .17; Fig. S1). Taken together, these findings suggest that hand-selective regions in LOTC and IPS represent how to grasp tools for use and that these effects are not simply due to textural or size differences between the stimuli used or actions performed.

Finally, we repeated the classification procedures using whole-brain searchlights (48; see Materials and Methods) to examine whether other brain regions represent how to appropriately grasp tools. As before, decoding accuracy from the tool classification (typical vs. atypical) was contrasted with that from the non-tool classifier (left vs. right), this time producing a difference map (Fig. 3; SI Table 3). Significantly higher decoding accuracy was found for tools, relative to biomechanically matched actions with non-tools, in a cluster within the left anterior temporal

cortex comprising the Superior/Middle Temporal (STG; MTG) and Parahippocampal Gyri (PHG). Additional clusters were found in the right Fusiform Gyrus (FG), anterior Superior Parieto-Occipital Cortex (aSPOC) and posterior Superior Temporal Sulcus (pSTS). No cluster of activity demonstrated higher decoding accuracy in the reverse direction, that is, for non-tools higher than tools.

DISCUSSION

Most neuroimaging experiments that investigate how tools and their associated actions are represented in the brain use visual paradigms where objects and body parts are displayed as 2D images and no real movements are performed (8). These studies have discovered a tight anatomical and functional relationship between hand- and tool-selective areas in LOTC and IPS, thought to reflect action-related processing however this was yet to be directly tested (27,28,29,36,37,49). For the first time, we tested whether independently visually-defined category-selective areas were sensitive to real action properties involving 3D tools. We found that representations about whether a 3D tool is being grasped appropriately for use were decodable from hand-selective areas (LOTC-Hand and IPS-Hand), but not from partially overlapping tool-, object-, or body-selective areas.

Our results indicate that visual hand-selective cortex contributes to the performance of actual hand movements with 3D tools. Furthermore, since these motor-relevant neural representations were detected exclusively for actions with tools (but not for biomechanically matched actions with control non-tools), our results reveal critical features of sensorimotor processing in hand-selective visual areas. First, their representations are sensitive to concepts acquired through experience (i.e., knowing how to grasp tools appropriately is a learnt skill; 50,51), fitting with evidence showing that learning about how to manipulate tools (e.g., 52). or even using this knowledge (35,42,53), affects LOTC and IPS activity. Second, information processed by hand-selective cortex is represented in an abstract format beyond low level properties (e.g., basic kinematics), since no significant decoding was found for grip size. This resembles reports that tool-selective areas in pMTG/LOTC and IPS represent abstract action goals (reach vs. grasp) regardless of biomechanics (26; also see 54), albeit our findings were observed for hand-selective areas only. Third, our study shows that these high-level representations are automatically evoked (25,51,55); as throughout the real-action fMRI task there was no explicit requirement to use the tools and participants were never told that we were investigating ‘tools’. Here for the first time we demonstrate that these principles, frequently described to support tool-use (7,18,56,57,58,59,60,61), apply to brain areas specialised for representing the human hand, our primary *tool* for interacting with the world.

An intriguing aspect of our results is the lack of decoding in tool-selective regions, even though these areas sharing voxels with hand-selective ROIs. Thus, despite their anatomical overlap, regions that respond to hands appear to be functionally distinct from tool-selective

regions (see 27; 37). Highlighting the robustness of this category-selective difference between tool and hand-selective regions, this dissociation was persistent across LOTC and IPS ROIs: successful decoding of grasp typicality for tools could be achieved in hand-selective and not tool-selective regions. This is the first evidence that visually-defined hand- and tool-selective regions code different information. Importantly, this pattern of results is unlikely to be driven by differences in ROI radius (e.g., 62) since the difference between hand- and tool-selective ROI size was negligible (mean voxel difference: IPS: 29; LOTC: 4). In fact, if category-related results were merely caused by ROI size, then significant decoding should have also been observed in LOTC-Object, because this region was much larger than the other LOTC ROIs (see Table S1). Alternatively, successful decoding in hand- (but not tool-) selective areas may reflect the fact that in our study the task required simply grasping-to-touch the tools, rather than utilising them. That is, coding in category-selective areas might operate in an effector-dependent manner, akin to how tool-selective pMTG/LOTC codes the type of action being performed when holding a pair of tongs, but not if being performed by the hand alone (26). In line with this interpretation, neural representations in LOTC-Hand of one-handed amputees are also known to become richer as prosthetic usage increases (63), which, again, indicates that the representations in hand-selective cortex depend on effector use. An alternative, but not mutually exclusive, possibility is that only tool-use actions elicit tool-selective representations (see 64 for distinct lesion sites associated with grasping vs. using tools) because of the cognitively taxing demands of these complex actions that rely on retrieving knowledge about manipulation hierarchies (65) and the laws that constrain object movement (66). In either case, the absence of significant decoding of tool manipulation in tool-selective cortex challenges the popular interpretation that brain activation for viewing tool pictures is a reflection of sensorimotor processing linked to tool manipulation (11,12,13,15,67, also see 18).

Whole-brain searchlight analysis further indicated that right pSPOC and pSTS and left anterior temporal cortex (ATC) also coded how to grasp tools appropriately for use. In line with this, increased grey matter density has been found in pSPOC and pSTS after action practice, including tool-use (68,69). The ATC, however, is traditionally thought to play a critical role in the processing of conceptual knowledge (70) with lesions or Transcranial Magnetic Stimulation (TMS) to this area impairing tasks that rely on retrieving information about a tool's function, but not how it is handled (71,72,73). Nevertheless, in line with our results, two recent studies using tool pictures also found that tool manipulation-related information can be decoded from the ATC (74,75). Clarifying specific roles of the regions identified here will be an important next step in understanding how the brain achieves complex tool-use and is well suited for connectivity approaches (76,77,78).

In conclusion, parietal and occipital visual regions specialised for representing hands, but not tools, as well as additional regions such as ATC, code how to appropriately grasp 3D tools for use. These findings raise novel questions about why overlapping hand- and tool-selective

regions are functionally distinct and begin to uncover which brain regions evolved to support tool-use, a defining feature of our species. Measuring hand-selectivity in visual areas could prove a fruitful avenue for monitoring motor rehabilitation outcomes.

MATERIALS AND METHOD

Participants. Twenty healthy participants (11 males) completed the real action fMRI experiment followed by an additional visual localizer experiment on a separate day. Data from one participant (male) was excluded from statistical analysis due to excessive head movements during the real action experiment (i.e., translation and rotation exceeded 1.5mm and 1.5° rotation) leaving a total sample of 19 participants (mean age = 23 years ± 4.2 years; age range = 18 - 34). All participants had normal or corrected-to-normal vision, no history of neurological or psychiatric disorders, were right-handed (79) and gave written consent in line with procedures approved by the ethics committee of the University of East Anglia.

Stimuli and Apparatus. A set of three common kitchen tools (knife, spoon and pizzacutter) and non-tool control bars were designed (Autodesk Inc.) and 3D-printed (Objet30 Desktop) in VeroWhite material (Statasys; Fig. 1A). Tools had identical handles with different functional-ends attached. Non-tools were comprised of three cylindrical shapes (adapted from 43) that had dimensions matching the handle, neck and functional-end of the tool they controlled for (for measurements see SI Materials and Methods). Each tool and non-tool pair were also carefully matched for elongation (e.g., 14). The non-tool control bars were chosen, instead of scrambled tools, to avoid familiarity confounds and thus, our control objects were familiar, but had no specific associated function. To reduce their variability and to match kinematic requirements when grasping the tool and non-tool pairs (i.e., grip aperture size and reach distance), a small black sticker was placed at pre-specified locations to indicate grasp points (80). Objects were secured to slots placed onto black pedestals used for stimulus presentation.

In a completely darkened room, participants were scanned in a head-tilted configuration that allowed direct viewing of the workspace and 3D stimuli without the use of mirrors (SI Materials and Methods; Fig. 1B). Objects were placed by an experimenter on a turntable above the participant's pelvis and were only visible when illuminated (45,51,80,81,82; Fig. 1B). For stimulus presentation, the workspace and object were illuminated from the front using a bright white Light Emitting Diode (LED) attached to a flexible plastic stalk (Loc-line, Lockwood Products; Fig. 1B). To control for eye movements, participants were instructed to fixate a small red LED throughout data collection which was positioned above and behind objects such that they appeared in the lower visual field (81; see SI Materials and Methods). Throughout the experiment, participants' right eye and arm movements were recorded using two MR-compatible infrared-sensitive cameras (MRC Systems GmbH) that allowed us to exclude errors by verifying that participants performed the correct grasping movement (hand camera; Fig. 1B) and

maintained fixation (eye camera; Fig. 1B; SI Materials and Methods). The likelihood of motion artefacts related to grasping was reduced by restraining the upper-right arm and providing support with additional cushions so that movements were performed by flexion around the elbow only. Auditory instructions were delivered to the participants through Earphones (Sensimetrics MRI-Compatible Insert Earphones Model S14, USA).

Real action experimental design. We used a powerful block-design fMRI paradigm, to maximise the contrast-to-noise ratio and generate a reliable estimate of the average response pattern (83; Fig. 1C), while also improving detection of blood oxygenation level-dependent (BOLD) signal changes without significant interference from artefacts during overt movement (84). A block began with an auditory instruction ('Left' or 'Right'; 0.5s) specifying which side of the upcoming object to grasp. During the ON-block (10s), the object was briefly illuminated for 0.25s five consecutive times (within 2s intervals) cueing the participant to grasp with a right-handed precision grip (i.e., index finger and thumb) along the vertical axis. Between actions, participants returned their hand to a "home" position with their right hand closed in a fist on their chest (see Fig. 1B). This brief object flashing presentation cycle during ON-blocks has been shown to maximise the signal-to-noise ratio in previous perceptual decoding experiments (85,86) and eliminates the sensory confound from viewing hand movements (81,87). An OFF-block (10s), followed the stimulation block, where the workspace remained dark and the experimenter prepared the next stimulus. A single fMRI run included 16 blocks involving the four grasping conditions (i.e., typical tool, atypical tool, right non-tool and left non-tool) each with three repetitions (one per exemplar; every object was presented twice and grasped on each side once). An additional foil tool and a foil non-tool were presented on the remaining four blocks per run, but not analysed as they were not biomechanically matched. On average participants completed six runs (minimum five, maximum seven) for a total of 18 repetitions per grasping condition. Block orders were pseudorandomised such that conditions were never repeated (two-back) and were preceded an equal amount of times by other conditions. Each functional scan lasted 356s, inclusive of start / end baseline fixation periods (14s). Each experimental session lasted ~2.25 hours (including setup, task practise and anatomical scan). Prior to the fMRI experiment, participants were familiarised with the setup and practiced the grasping tasks in a separate lab session (30 minutes) outside of the scanner.

MRI Acquisition. The BOLD fMRI measurements were acquired using a 3T wide bore GE-750 Discovery MR scanner (SI Materials and Methods). To achieve a good signal to noise ratio during the real action fMRI experiment, the posterior half of a 21-channel receive-only coil was tilted and a 16-channel receive-only flex coil was suspended over the anterior-superior part of the skull (see Fig. 1B). A T2*-weighted single-shot gradient Echo-Planer Imaging (EPI) sequence was used throughout the real action experiment to acquire 178 functional MRI volumes (Time to

Repetition [TR] = 2000ms; Voxel Resolution [VR] = 3.3 x 3.3 x 3.3mm; Time to Echo [TE] = 30ms; Flip Angle [FA] = 78°; Field of View [FOV] = 211x 211mm; Matrix Size [MS] = 64 x 64) that comprised 35 oblique slices (no gap) acquired at 30° with respect to AC-PC, to provide near whole brain coverage. A T1-weighted anatomical image with 196 slices was acquired at the beginning of the session using BRAVO sequences (TR = 2000ms; TE = 30ms; FOV = 230mm x 230mm x 230mm; FA = 9°; MS = 256 x 256; Voxel size = 0.9 x 0.9 x 0.9mm).

Visual Localizer. On a separate day from the real action experiment, participants completed a Bodies, Chairs, Tools and Hands visual localizer (adapted from 27,28,29). A standard coil configuration was used for the visual localizer session. For details see SI Materials and Methods.

Data Preprocessing. Preprocessing of the raw functional datasets and ROI definitions were performed using BrainVoyager QX [version 2.8.2] (Brain Innovation, Maastricht, The Netherlands). Anatomical data were transformed to Talairach space and fMRI time series were preprocessed using standard parameters (no smoothing) before being coaligned to an anatomical dataset (SI Materials and Methods). Timeseries from the real action and localizer experiments were subjected to a general linear model with predictors per condition of interest, as to estimate activity patterns for MVPA and defining ROIs, respectively (SI Materials and Methods).

Pattern Classification. We trained two linear pattern classifiers (linear SVM), independently for tool and control non-tool trials, to learn the mapping between a set of brain-activity patterns and the type of grasp being performed (86; SI Materials and Methods). We then tested the classifiers on an independent set of test data (leave one run out cross-validation). These procedures were performed within single participants using voxel beta-weight input (per block) from the independently defined visual localizer ROIs (see Fig. S2 for raw beta weights) and repeated using whole-brain searchlights (88,89; SI Materials and Methods).

ACKNOWLEDGEMENTS. We thank Jenna Green, Richard Greenwood, Holly Weaver, Iwona Szymura and Emmeline Mottram for support in data collection, Derek Quinlan for building the real action set-up and Stefania Bracci for sharing the visual localizer stimuli. This work was funded by grant (184/14) from the BIAL Foundation awarded to S. Rossit & F.W. Smith.

COMPETING INTERESTS. The authors have no competing interests to disclose.

AUTHOR CONTRIBUTIONS. S.R., E.K. and F.W.S conceptualised the study; E.K., C.M., D.T. and S.R. collected data; E.K., J.S., F.W.S and S.R. analysed data; E.K., F.W.S. and S.R. wrote the manuscript; S.R. and F.W.S. acquired funding.

REFERENCES

1. Ambrose, S. H. (2001). Paleolithic technology and human evolution. *Science*, **291**(5509), 1748-1753.
2. Johnson-Frey, S. H. (2004). The neural bases of complex tool use in humans. *Trends Cogn Sci*, **8**(2), 71-78.
3. Osiurak, F., Lesourd, M., Delporte, L., & Rossetti, Y. (2018). Tool use and generalized motor programs: we all are natural born poly-dexters. *Sci Rep*, **8**(1), 1-7.
4. Kanwisher, N. (2010). Functional specificity in the human brain: a window into the functional architecture of the mind. *Proc Natl Acad Sci USA,* **107**(25), 11163-11170.
5. DiCarlo, J. J., Zoccolan, D., & Rust, N. C. (2012). How does the brain solve visual object recognition?. *Neuron*, **73**(3), 415-434.
6. Castiello, U. (2005). The neuroscience of grasping. *Nat Rev Neurosci,* **6**(9), 726-736.
7. Gallivan, J. P., & Culham, J. C. (2015). Neural coding within human brain areas involved in actions. *Curr Opin Neurobiol,* **33**, 141-149.
8. Lewis, J. W. (2006). Cortical networks related to human use of tools. *The neuroscientist,* **12**(3), 211-231.
9. Valyear, K. F., Fitzpatrick, A. M., & McManus, E. F. (2017). “The neuroscience of human tool use” in *Evolution of Nervous Systems*. Kaas, J. (Ed.), pp. 341-353, Elsevier, Oxford.
10. Osiurak, F., & Heinke, D. (2018). Looking for intoolligence: A unified framework for the cognitive study of human tool use and technology. *Am Psychol,* **73**(2), 169-185.
11. Martin, A., Wiggs, C. L., Ungerleider, L. G., & Haxby, J. V. (1996). Neural correlates of category-specific knowledge. *Nature,* **379**(6566), 649-652.
12. Mahon, B. Z., et al., (2007). Action-related properties shape object representations in the ventral stream. *Neuron,* **55**(3), 507-520.
13. Fang, F., & He, S. (2005). Cortical responses to invisible objects in the human dorsal and ventral pathways. *Nat Neurosci,* **8**(10), 1380-1385.
14. Almeida, J., Mahon, B. Z., Nakayama, K., & Caramazza, A. (2008). Unconscious processing dissociates along categorical lines. *Proc Natl Acad Sci USA*, **105**(39), 15214-15218.
15. Grafton, S. T., Fadiga, L., Arbib, M. A., & Rizzolatti, G. (1997). Premotor cortex activation during observation and naming of familiar tools. *Neuroimage,* **6**(4), 231-236.
16. Martin, A., & Chao, L. L. (2001). Semantic memory and the brain: structure and processes. *Curr Opin Neurobiol,* **11**(2), 194-201.
17. Johnson-Frey, S. H. (2004). The neural bases of complex tool use in humans. *Trends Cogn Sci,* **8**(2), 71-78.
18. Mahon, B. Z., & Caramazza, A. (2009). Concepts and categories: a cognitive neuropsychological perspective. *Annu Rev Psychol,* **60**, 27-51.

19. Martin, A. (2016). GRAPES—Grounding representations in action, perception, and emotion systems: How object properties and categories are represented in the human brain. *Psychon Bull Rev*, **23**(4), 979-990.
20. Bach, P., Peelen, M. V., & Tipper, S. P. (2010). On the role of object information in action observation: an fMRI study. *Cereb Cortex,* **20**(12), 2798-2809.
21. Dinstein, I., Thomas, C., Behrmann, M., & Heeger, D. J. (2008). A mirror up to nature. *Curr Biol,* **18**(1), R13-R18.
22. Warrington, E. K., & Shallice, T. (1984). Category specific semantic impairments. *Brain,* **107**(3), 829-853.
23. Barsalou, L. W. (2008). Grounded cognition. *Annu Rev Psychol,* **59**, 617-645.
24. Patterson, K., Nestor, P. J., & Rogers, T. T. (2007). Where do you know what you know? The representation of semantic knowledge in the human brain. *Nat Rev Neurosci,* **8**(12), 976-987.
25. Valyear, K. F., Cavina-Pratesi, C., Stiglick, A. J., & Culham, J. C. (2007). Does tool-related fMRI activity within the intraparietal sulcus reflect the plan to grasp? *Neuroimage,* **36**, T94-T108.
26. Gallivan, J. P., McLean, D. A., Valyear, K. F., & Culham, J. C. (2013). Decoding the neural mechanisms of human tool use. *Elife*, **2**, e00425.
27. Bracci, S., Cavina-Pratesi, C., Ietswaart, M., Caramazza, A., & Peelen, M. V. (2012). Closely overlapping responses to tools and hands in left lateral occipitotemporal cortex. *J Neurophysiol,* **107**(5), 1443-1456.
28. Bracci, S., & Peelen, M. V. (2013). Body and object effectors: the organization of object representations in high-level visual cortex reflects body–object interactions. *J Neurosci***,** **33**(46), 18247-18258.
29. Bracci, S., & de Beeck, H. O. (2016). Dissociations and associations between shape and category representations in the two visual pathways. *J Neurosci,* **36**(2), 432-444.
30. Coggan, D. D., Liu, W., Baker, D. H., & Andrews, T. J. (2016). Category-selective patterns of neural response in the ventral visual pathway in the absence of categorical information. *Neuroimage*, **135**, 107-114.
31. Konkle, T., & Caramazza, A. (2013). Tripartite organization of the ventral stream by animacy and object size. *J Neurosci,* **33**(25), 10235-10242.
32. Long, B., Yu, C. P., & Konkle, T. (2018). Mid-level visual features underlie the high-level categorical organization of the ventral stream. *Proc Natl Acad Sci USA,* **115**(38), E9015-E9024.
33. Perini, F., Caramazza, A., & Peelen, M. V. (2014). Left occipitotemporal cortex contributes to the discrimination of tool-associated hand actions: fMRI and TMS evidence. *Front Hum Neurosci,* 591.

34. Palser, E., & Cavina-Pratesi, C. (2018). Left lateral occipito-temporal cortex encodes compatibility between hands and tools: an fMRI adaptation study. 10.31234/osf.io/kbjw4 (15 June 2019).
35. Bracci, S., Caramazza, A., & Peelen, M. V. (2018). View-invariant representation of hand postures in the human lateral occipitotemporal cortex. *NeuroImage,* 1**81**, 446-452.
36. Peelen, M. V., et al., (2013). Tool selectivity in left occipitotemporal cortex develops without vision. *J Cogn Neurosci*, **25**(8), 1225-1234.
37. Striem-Amit, E., Vannuscorps, G., & Caramazza, A. (2017). Sensorimotor-independent development of hands and tools selectivity in the visual cortex. *Proc Natl Acad Sci USA,* **114**(18), 4787-4792.
38. Astafiev, S. V., Stanley, C. M., Shulman, G. L., & Corbetta, M. (2004). Extrastriate body area in human occipital cortex responds to the performance of motor actions. *Nat Neurosci,* **7**(5), 542-548.
39. Peelen, M. V., & Downing, P. E. (2005). Is the extrastriate body area involved in motor actions? *Nat Neurosci,* **8**(2), 125-125.
40. Orlov, T., Makin, T. R., & Zohary, E. (2010). Topographic representation of the human body in the occipitotemporal cortex. *Neuron,* **68**(3), 586-600.
41. Johnson-Frey, S. H., et al., (2003). Actions or hand-object interactions? Human inferior frontal cortex and action observation. *Neuron,* **39**(6), 1053-1058.
42. Valyear, K. F., & Culham, J. C. (2010). Observing learned object-specific functional grasps preferentially activates the ventral stream. *J Cogn Neurosci,* **22**(5), 970-984.
43. Brandi, M. L., Wohlschläger, A., Sorg, C., & Hermsdörfer, J. (2014). The neural correlates of planning and executing actual tool use. *J Neurosci,* **34**(39), 13183-13194.
44. Wiggett, A. J., & Downing, P. E. (2011). Representation of action in occipito-temporal cortex. *J Cogn Neurosci,* **23**(7), 1765-1780.
45. Gallivan, J. P., Cant, J. S., Goodale, M. A., & Flanagan, J. R. (2014). Representation of object weight in human ventral visual cortex. *Curr Biol,* **24**(16), 1866-1873.
46. Hutchison, R. M., Culham, J. C., Everling, S., Flanagan, J. R., & Gallivan, J. P. (2014). Distinct and distributed functional connectivity patterns across cortex reflect the domain-specific constraints of object, face, scene, body, and tool category-selective modules in the ventral visual pathway. *Neuroimage,* **96**, 216-236.
47. Fabbri, S., Stubbs, K. M., Cusack, R., & Culham, J. C. (2016). Disentangling representations of object and grasp properties in the human brain. *J Neurosci,* **36**(29), 7648-7662.
48. Kriegeskorte, N., Goebel, R., & Bandettini, P. (2006). Information-based functional brain mapping. *Proc Natl Acad Sci USA,* **103**(10), 3863-3868.
49. Maimon Mor, R. O., & Makin, T. R. (2020). Is an artificial limb embodied as a hand? *Brain* decoding in prosthetic limb users. PLoS Biol, **18**(6), e3000729.

50. Martin, A. (2007). The representation of object concepts in the brain. *Annu. Rev. Psychol.,* **58**, 25-45.
51. Valyear, K. F., Gallivan, J. P., McLean, D. A., & Culham, J. C. (2012). fMRI repetition suppression for familiar but not arbitrary actions with tools. *J Neurosci,* **32**(12), 4247-4259.
52. Weisberg, J., Van Turennout, M., & Martin, A. (2007). A neural system for learning about object function. *Cereb Cortex,* **17**(3), 513-521.
53. Styrkowiec, P. P., Nowik, A. M., & Króliczak, G. (2019). The neural underpinnings of haptically guided functional grasping of tools: an fMRI study. *Neuroimage,* **194**, 149-162.
54. Jacobs, S., Danielmeier, C., & Frey, S. H. (2010). Human anterior intraparietal and ventral premotor cortices support representations of grasping with the hand or a novel tool. *J Cogn Neurosci,* **22**(11), 2594-2608.
55. Grèzes, J., Tucker, M., Armony, J., Ellis, R., & Passingham, R. E. (2003). Objects automatically potentiate action: an fMRI study of implicit processing. *Eur J Neurosci,* **17**(12), 2735-2740.
56. Gibson J. J. (1979) *The ecological approach to visual perception.* Boston: Houghton Mifflin.
57. Imamizu, H., Kuroda, T., Miyauchi, S., Yoshioka, T., & Kawato, M. (2003). Modular organization of internal models of tools in the human cerebellum. *Proc Natl Acad Sci USA,* **100**(9), 5461-5466.
58. Maravita, A., & Iriki, A. (2004). Tools for the body (schema). Trends Cogn Sci, **8**(2), 79-86.
59. Frey, S. H. (2008). Tool use, communicative gesture and cerebral asymmetries in the modern human brain. *Philos Trans R Soc Lond B Biol Sci,* **363**(1499), 1951-1957.
60. Umiltà, M. A., et al., (2008). When pliers become fingers in the monkey motor system. *Proc Natl Acad Sci USA,* **105**(6), 2209-2213.
61. Lingnau, A., & Downing, P. E. (2015). The lateral occipitotemporal cortex in action. *Trends Cogn Sci,* **19**(5), 268-277.
62. Etzel, J. A., Zacks, J. M., & Braver, T. S. (2013). Searchlight analysis: promise, pitfalls, and potential. *Neuroimage,* **78**, 261-269.
63. Van den Heiligenberg, F. M., et al., (2018). Artificial limb representation in amputees. *Brain,* **141**(5), 1422-1433.
64. Randerath, J., Goldenberg, G., Spijkers, W., Li, Y., & Hermsdörfer, J. (2010). Different left brain regions are essential for grasping a tool compared with its subsequent use. *Neuroimage,* **53**(1), 171-180.
65. Buxbaum, L. J. (2017). Learning, remembering, and predicting how to use tools: Distributed neurocognitive mechanisms: Comment on Osiurak and Badets (2016). *Psychol Rev,* **124**(3), 346-360.
66. Fischer, J., Mikhael, J. G., Tenenbaum, J. B., & Kanwisher, N. (2016). Functional neuroanatomy of intuitive physical inference. *Proc Natl Acad Sci USA,* **113**(34), E5072-E5081.

67. Martin, A., & Chao, L. L. (2001). Semantic memory and the brain: structure and processes. *Curr Opin Neurobiol,* **11**(2), 194-201.
68. Scholz, J., Klein, M. C., Behrens, T. E., & Johansen-Berg, H. (2009). Training induces changes in white-matter architecture. *Nat Neurosci,* **12**(11), 1370-1371.
69. Quallo, M. M., et al., (2009). Gray and white matter changes associated with tool-use learning in macaque monkeys. *Proc Natl Acad Sci USA*, **106**(43), 18379-18384.
70. Ralph, M. A. L., Sage, K., Jones, R. W., & Mayberry, E. J. (2010). Coherent concepts are computed in the anterior temporal lobes. *Proc Natl Acad Sci USA,* **107**(6), 2717-2722.
71. Martin, M., et al., (2016). Differential roles of ventral and dorsal streams for conceptual and production-related components of tool use in acute stroke patients. *Cereb Cortex,* **26**(9), 3754-3771.
72. Ishibashi, R., Ralph, M. A. L., Saito, S., & Pobric, G. (2011). Different roles of lateral anterior temporal lobe and inferior parietal lobule in coding function and manipulation tool knowledge: evidence from an rTMS study. *Neuropsychologia,* **49**(5), 1128-1135.
73. Hodges, J. R., Spatt, J., & Patterson, K. (1999). "What" and "how": evidence for the dissociation of object knowledge and mechanical problem-solving skills in the human brain. *Proc Natl Acad Sci USA,* **96**(16), 9444-9448.
74. Peelen, M. V., & Caramazza, A. (2012). Conceptual object representations in human anterior temporal cortex. *J Neurosci,* **32**(45), 15728-15736.
75. Chen, Q., Garcea, F. E., & Mahon, B. Z. (2016). The representation of object-directed action and function knowledge in the human brain. *Cereb Cortex,* **26**(4), 1609-1618.
76. Noppeney, U., Price, C. J., Penny, W. D., & Friston, K. J. (2006). Two distinct neural mechanisms for category-selective responses. *Cereb Cortex,* **16**(3), 437-445.
77. Malone, P. S., Glezer, L. S., Kim, J., Jiang, X., & Riesenhuber, M. (2016). Multivariate pattern analysis reveals category-related organization of semantic representations in anterior temporal cortex. *J Neurosci,* **36**(39), 10089-10096.
78. Garcea, F. E., & Buxbaum, L. J. (2019). Gesturing tool use and tool transport actions modulates inferior parietal functional connectivity with the dorsal and ventral object processing pathways. *Hum Brain Mapp,* **40**(10), 2867-2883.
79. Oldfield, R.C. (1971). The assessment and analysis of handedness: The Edinburgh inventory. *Neuropsychologia*, **9**(1), 97-113.
80. Gallivan, J. P., McLean, D. A., Flanagan, J. R., & Culham, J. C. (2013). Where one hand meets the other: limb-specific and action-dependent movement plans decoded from preparatory signals in single human frontoparietal brain areas. *J Neurosci,* **33**(5), 1991-2008.
81. Rossit, S., McAdam, T., Mclean, D. A., Goodale, M. A., & Culham, J. C. (2013). fMRI reveals a lower visual field preference for hand actions in human superior parieto-occipital cortex (SPOC) and precuneus. *Cortex*, **49**(9), 2525-2541.

82. Snow, J. C., et al., (2011). Bringing the real world into the fMRI scanner: Repetition effects for pictures versus real objects. *Sci Rep,* **1**, 130.

83. Mur, M., Bandettini, P. A., & Kriegeskorte, N. (2009). Revealing representational content with pattern-information fMRI—an introductory guide. *Soc Cogn Affect Neurosci,* **4**(1), 101-109.

84. Birn, R. M., Cox, R. W., & Bandettini, P. A. (2004). Experimental designs and processing strategies for fMRI studies involving overt verbal responses. *Neuroimage,* **23**(3), 1046-1058.

85. Kay, K. N., Naselaris, T., Prenger, R. J., & Gallant, J. L. (2008). Identifying natural images from human brain activity. *Nature*, **452**(7185), 352-355.

86. Smith, F. W., & Muckli, L. (2010). Nonstimulated early visual areas carry information about surrounding context. *Proc Natl Acad Sci USA*, **107**(46), 20099-20103.

87. Monaco, S., Sedda, A., Cavina-Pratesi, C., & Culham, J. C. (2015). Neural correlates of object size and object location during grasping actions. *European J Neurosci,* **41**(4), 454-465.

88. Pereira, F., & Botvinick, M. (2011). Information mapping with pattern classifiers: a comparative study. *Neuroimage,* **56**(2), 476-496.

89. Smith, F.W. & Goodale, M.A. (2015). Decoding visual object categories in early somatosensory cortex. *Cerebral Cortex*, **25**(4), 1020-1031.

FIGURES

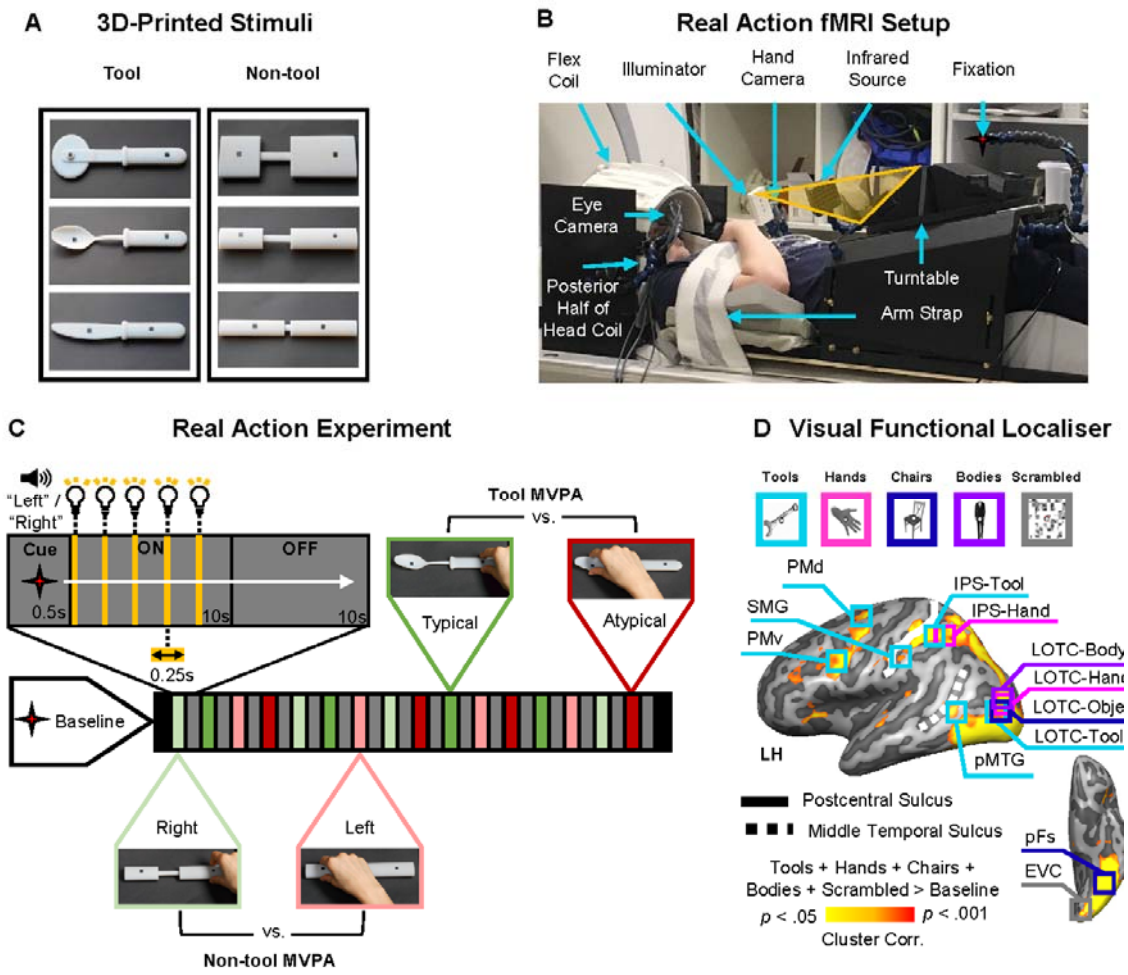

Figure 1. Experimental set-up and design. (**A**) Real action 3D-printed tool and non-tool control object pairs (black markers on objects indicate grasp points) matched for elongation, width and depth. (**B**) Side view of real action participant set-up used to present 3D objects at grasping distance (without the use of mirrors). Red star indicates fixation LED. The hand is shown at its starting position. (**C**) Timing and grasping tasks from subject's point of view. During the 10s ON-block the object was illuminated 5 times cueing the participant to grasp the object each time by its left or right sides (as per preceding auditory cue) with the right hand. This was followed by a 10s OFF-block involving no stimulation where the workspace remained dark. For MVPA, we treated tool and non-tool trials independently, where for the tools only, right- and left-sided grasps were typical and atypical grasps respectively (based on handle orientation). (**D**) Visual functional localizer experiment tools, hands, chairs, bodies and scrambled exemplar stimuli. For each individual participant independent ROIs were defined for MVPA. The representative ROI locations are displayed on a group activation contrast map from the visual localizer [All conditions > (Baseline*5)] projected onto a left hemisphere cortical surface reconstruction of a reference brain (COLIN27 Talairach) available from the neuroElf package (http://neuroelf.net).

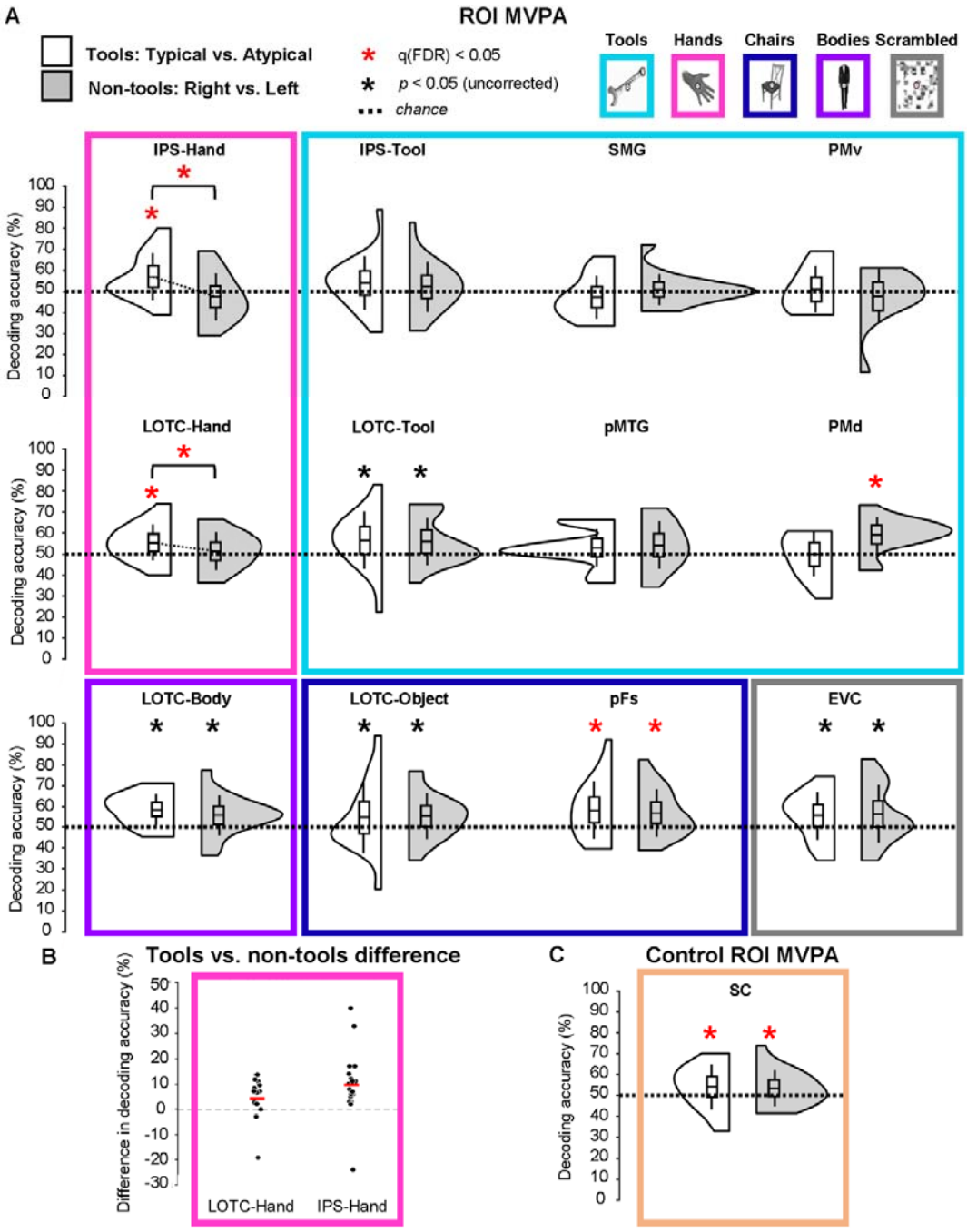

Figure 2. Grasp type decoding results in left hemisphere ROIs. (**A**) Violin plots of MVPA data from visual localizer ROIs for the typical vs. atypical classification of grasping tools (white violins) and, non-tool control grasping (right vs. left decoding; grey violins). Box plot centre lines are mean decoding accuracy while their edges and whiskers show ±1SD and ±2SEM, respectively. Decoding accuracies of typical vs. atypical grasping in IPS and LOTC hand-selective cortex (pink) are significantly greater-than-chance for tools, but not non-tools. (**B**) Differences of tool vs. non-tool decoding accuracy of typical vs. atypical grasping (or right vs. left) per participant for hand-selective ROIs (red line = mean decoding accuracy difference). (**C**) Violin plot of MVPA data for control ROI in

somatosensory cortex (SC) based on an independent contrast (all actions > baseline) from real action experiment showing significant decoding of grasp type for both tools and non-tools. Red asterisks show FDR-corrected results while black asterisks show uncorrected data.

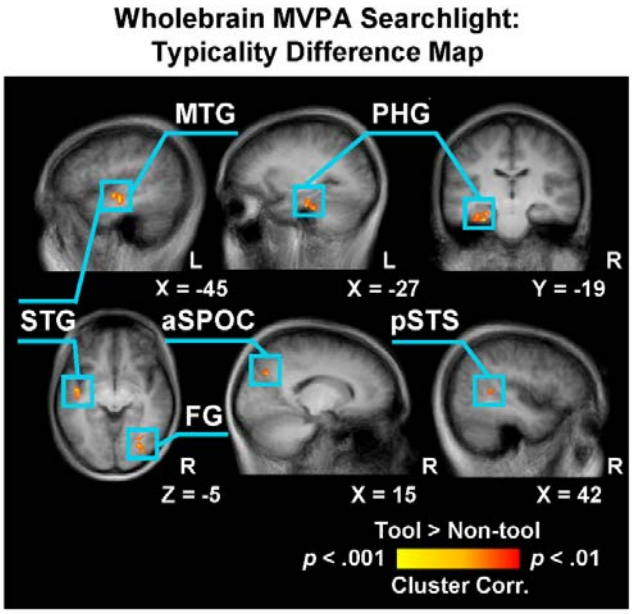

Figure 3. Whole-brain searchlight MVPA typicality difference map. Data shown on the group average structural MRI. Tool and non-tool typicality decoding accuracies were calculated independently in searchlight analyses for each participant then subtracted to generate the difference map between tools and non-tools decoding. To correct for multiple comparisons cluster correction was used (voxelwise P<0.01, cluster P<0.05; cluster size = 10 voxels).